

Microwave-based preparation and characterization of Fe-cored carbon nanocapsules with novel stability and super electromagnetic wave absorption performance

Yican Wang ^a, Wenlong Wang ^{a,*}, Jing Sun ^{a,**}, Chenggong Sun ^{b,***}, Yukun Feng ^a,
Zhe Li ^a

^a *National Engineering Laboratory of Coal-fired Pollutants Emission Reduction, School of Energy and Power Engineering, Shandong University, Jinan 250061, China*

^b *Faculty of Engineering, University of Nottingham, University Park, Nottingham NG7 2RD, UK*

HIGHLIGHTS

- Microwave-metal discharge used for the preparation of Fe@CNCs.
- Exceedingly high degree of graphitization and excellent material integrity achieved.
- Novel thermo-oxidative stability and super anti-corrosion performance obtained.
- The advanced material demonstrates desirable absorption of EMW across wide-range of bandwidth.

ABSTRACT

Microwave-metal discharge was proposed as a facile methodology to prepare unique Fe-cored carbon nanocapsules (Fe@CNCs) with high purity, novel stability and extraordinary electromagnetic wave (EMW) absorption performance. The effect of microwave power, irradiation time and cyclohexane/ferrocene ratio on the production

* Corresponding author.

** Corresponding author.

*** Corresponding author.

E-mail address: wwenlong@sdu.edu.cn (W. Wang), sunj7@sdu.edu.cn (J. Sun),
Cheng-Gong.Sun@nottingham.ac.uk (C. Sun).

of Fe@CNCs was examined and the properties of the nanocapsules, such as their Fe content, phase, **yield**, degree of graphitization and associated microstructures were investigated in detail. It was found that the prepared Fe@CNCs, which can easily be separated from the reaction system, displayed exceedingly high electromagnetic wave (EMW) absorption performance over the 2-18 GHz range. At the minimal reflection loss (RL) values over -10 dB, the EMW absorption bandwidth can reach up to 13.8 GHz with an absorber thickness of 1.5-5 mm. In addition, novel thermo-oxidative stability and super anti-corrosion property were also obtained for the Fe@CNCs as no signs of any corrosion or oxidative degradation loss were observed from the accelerated degradation tests in air and acid at temperatures up to 420 °C. The exceedingly high EMW absorption performance coupled with the superior anti-degradation and anti-corrosion properties of the prepared nanocomposite microcapsules highlights the novel capability of microwave-metal discharge in synthesizing advanced metal-cored nanocarbon microcapsules with promising application potentials in diverse fields, such as but not limited to microwave absorption, EM shielding and advanced separations etc.

Keywords: Fe-cored carbon nanocapsules, microwave-metal discharge, preparation, stability, electromagnetic wave absorption

1. Introduction

Nanocapsules are a class of nanocomposites with a unique core/shell structure with size ranging from a few nanometers to hundreds of nanometers. Due to their special optical, electrical, magnetic and catalytic properties[1, 2] and their promising application potentials in electromagnetic wave (EMW) absorption[3-5], battery technology[6-8],

catalyst[9, 10], biomedical[11] and electromagnetic (EM) shielding[12], how to develop metal-cored nanocapsules with robust performances have attracted intensive research activities over recent years. Nanocapsules with appropriate materials as being the shell can effectively protect the metal core from getting oxidized thus to improve their stability in hostile environment[13, 14]. A number of nanocapsules have been investigated, with the shell structures fabricated ranging from carbon materials[15, 16], boron nitride[17], conductive polymers (e.g. phosphates)[18] to metal or semiconductor oxides[19, 20]. Among them, carbon shell materials are considered ideal owing to their proper dielectric properties, low cost, easy access and good environmental stability. As a result, the carbon-based soft magnetic metal nanocapsules, which are often referred to as metal-cored carbon nanocapsules (M@CNCs) usually with Fe, Co, Ni and their alloys as the core, become a research of intensive interest because the exchange coupling effect at the heterogeneous interface can induce the aforementioned desirable properties that cannot be possibly achieved otherwise.

One of the novel properties of M@CNCs is their unparalleled performance in EMW absorption over single-substance materials owing to the unique core-shell structure. Magnetic metal nanoparticles have the characteristics of high saturation magnetization and shape anisotropy. Compared with micron magnetic metal particles, M@CNCs show higher magnetic permeability and magnetic loss in wide frequency ranges of gigahertz[21, 22]. As their characteristic particle sizes are 1~100 nm, lower than their skin depth in the EMW band, the restriction of eddy current effect can be furthermore avoided[23]. However, magnetic nanometals alone cannot achieve effective absorption

of EMW due to the limited achievable dielectric losses. Nevertheless, the existence of carbon shell can effectively solve this problem, thanks to their excellent conductivity and dielectric properties. In addition, the increase of electrical resistivity can also effectively improve the attenuation constant. It is the cross-coupling effects among magnetic loss and dielectric loss as well as the larger attenuation constant that jointly contribute to the enhanced EMW absorption performance of the M@CNCs.

Despite the superiorities, the practical applications of M@CNCs still faces major challenges or performance hurdles such as the lack of scalable production methodologies and the associated issues of product purity. Following the arc discharge method that was first used by Rouff et al, a variety of other preparation methods have been investigated, such as chemical vapor deposition (CVD), high temperature carbonization, pyrolysis, hydrothermal and explosion methodologies[1, 24-28]. Among these technologies, CVD appears to be the best available methodology at present but suffers from major drawbacks, such as the product purity and separation problems. Other technologies currently under development also face their own disadvantages. For instance, pyrolysis method benefits from process simplicity but the selection of appropriate precursors is the major challenge yet with high energy consumption and long preparation cycle whereas the complicated explosion methodology is almost impossible to operate and control with confidence. In addition to the shortcomings of preparation methodologies, the performance of the product also faced some problems. For example, carbon-encapsulated iron hybrids and graphite-coated FeNi nanoparticles synthesized by hydrothermal and arc-discharge methods are stable only in air and at

temperatures below 180 °C and 240 °C respectively, highlighting their relatively poor thermo-oxidative stability[9, 29]. In addition, the absorption bandwidth for a given absorber thickness of the M@CNCs prepared by arc-discharge plasma method with RL values exceeding -10 dB is narrow[30, 31], which limits the potentials of their applications. Therefore, more practical or effective technologies have to be developed. Microwave-metal (MW-M) discharge can potentially serve as a novel approach to fabricate high-performance M@CNCs, due to its capabilities in facilitating multiple effects to take place simultaneously, such as strong selective heating, photo-catalytic and plasma effects[32]. When metal with tips or sharp edges were exposed to the microwave field, intense discharge phenomena may occur. Our previous investigations have demonstrated the novel application potentials of microwave-metal discharge in eliminating toxic volatile organic emissions and associated mechanisms[33, 34]. It was then interestingly found that the decomposition of carbonaceous compounds was often accompanied by the formation of dense carbon fragments. The transient local high temperature with localized pressure in the discharge area, which can reach up to 3000 °C[35, 36], provide desirable conditions to facilitate the formation of density carbons with high degrees of graphitization.

Herein, the potential of using MW-M discharge as an approach to prepare iron-cored nanocapsules (Fe@CNCs) was for the first time explored, and the properties of the material were characterized using a variety of advanced characterization tools. To demonstrate the application potentials, the performance of this material for microwave absorption and EM shielding was evaluated with outstanding results.

2. Experimental section

2.1. Materials and sample preparation

All chemicals used, typically including cyclohexane, ethanol and concentrated nitric acid were mainly purchased from Aladdin Industrial Corporation (ferrocene) and Sinopharm Chemical Reagent Co. Ltd. (including cyclohexane, ethanol and concentrated nitric acid). The concentrated nitric acid was diluted to 3 mol/L by deionized water, as acid lotion. Nickel wires (1 mm in diameter and 3-6 mm in length) obtained from Shanghai Shen Long High Temperature Line were used to induce microwave discharges in a self-designed industrial microwave oven (300-4000 W, 2.45 GHz). High purity argon (99.999%) acted as a protective gas.

A purpose-built quartz reactor with high-purity quartz glass, which can provide the required microwave transparency, was used to synthesize the Fe@CNPs with microwave-metal discharge via a dissolution-precipitation mechanism. In brief, to prepare the Fe@CNPs, cyclohexane and ferrocene were first mixed at a pre-determined weight ratio (cyclohexane: ferrocene = 5:1, 10:1, 15:1, 20:1, 25:1 and 30:1) in a quartz tube and then the nickel wires (2 g) were added into the aqueous mixture. The selection of the ferrocene/cyclohexane ratio is based on two important factors, namely the solubility of ferrocene in cyclohexane and the minimal volume required to facilitate the materials synthesis for the given experimental conditions. The nickel wires with tips are used to induce the desirable discharge under microwave irradiation and the amount of nickel used is determined by the required level of MW-metal discharge required for a given volume of the reactants. The mixture was then subjected to ultrasonic dispersion

for 10 min before it was positioned in a quartz reactor. The reactor containing the mixture was then placed in the microwave oven and purged thoroughly with argon at 200 mL/min to create an oxygen-free environment. Then, the mixture was exposed to microwave irradiation at different power output levels (800, 1000, 1200, 1400, 1600, 1800, 2000, 2400 and 2600 W) for variable duration times (2, 2.5, 3, 3.5, 4, 4.5 and 5 min) in a continuous flow of argon at 200 ml/min. During microwave irradiation, strong discharge occurred at the tips of the nickel wires, and a series of chemical reactions took place in the mixed solution. After the microwave-metal discharge treatment under different conditions, the quartz tube turned black and the tips of some metal wires were melted. Then, the reactor was allowed to cool naturally down to ambient temperature in a flow of argon before the carbon formed was collected from the reactor. The collected carbon was then firstly washed for 3 h with dilute nitric acid (3 M) under vigorous stirring conditions to remove the residual ferrocene and incomplete coated iron nanoparticles, and this was followed by further washing with ethanol and deionized water to remove the amorphous carbon. The graphitized or purified Fe@CNCs was then obtained by drying the remaining solid residue in an oven at 80 °C for 6 h. In order to optimize the morphology and performance of the products, a series of samples were prepared by changing the microwave power, microwave irradiation time and mass ratio of raw materials according to the above experimental method. The samples prepared under different conditions were labelled as Ax-y-z where x refers to the microwave power out level, y the duration time and z the cyclohexane/ferrocene mass ratio. For instance, sample A1800-4-15 represents the sample prepared with a power output level

of 1800 W at a discharge duration time of 4 min and a cyclohexane/ferrocene ratio of 15.

2.2. Materials characterization

Phase and Structure: Powder X-ray diffractometer (XRD) (Rigaku D/MAX2500V diffractometer) with Cu K α radiation ($\lambda = 0.15406$ nm) was employed to determine the phase of the products. The graphitization degree and molecular structure of the samples was confirmed by Raman spectroscopy (Renishaw inVia) based on a He-Ne laser with a wavelength of 633 nm.

Morphology and Microstructure: The morphology and particle size of the products were investigated by thermal field scanning electron microscope (SEM) equipped with an energy dispersive spectrometer (EDS). The microstructure of the samples dispersed in a standard copper grids after ultrasonic dispersion in ethanol solvent was analyzed in detail by high resolution transmission electron microscopy (TEM, FEI).

Stability and Elemental Content Measurement: Thermogravimetric analysis (TGA) equipped with a simultaneous thermal analyzer was used to characterize the thermo-oxidative stability and elemental content of the prepared Fe@CNPs under an air flow of 100 ml/min at a heating rate of 10 °C/min.

Porosity: Pore size and Brunauer-Emmett-Teller (BET) specific surface area were measured by a Gas Sorption Analyzer Autosorb IQ after degassing treatment at 190 °C for 10 h.

Magnetic and EMW Absorption Performance: The vibrating sample magnetometer

(VSM) was used to measure the magnetic properties of samples at room temperature. Before determining the EM parameters (permittivity and permeability), the Fe@CNCs (30 wt%) and the paraffin mixture were first processed into a toroidal sample (7 mm outer diameter and 3.04 mm inner diameter). A vector network analyzer (Agilent PNA-N5244A) was then used to measure the EMW absorption performance of the sample at a frequency of 2-18 GHz.

3. Results and discussion

To investigate the porosity and the BET surface area of the Fe-cored nanocapsules, the N₂ adsorption-desorption experiment was carried out. The N₂ adsorption-desorption isotherm and pore size distribution curve are shown in Fig. 1. The isotherm is a typical type IV isotherm with a H3 type hysteresis according to the classification of IUPAC[37], being indicative of the slit-like mesopores that are created by the aggregates of platy particles namely the Fe-cored capsular nanocarbon particles. The nanocapsules has a specific surface area of 56.8 m²/g and pore volume of 0.19 cm³/g, with a single modal pore size distribution centred at about 10 nm. The BET surface area of the nano-capsules prepared with MW discharge is considerably larger than those of the same type of the reported nanocapsules prepared by other methodologies, such as GN-pFe₃O₄@ZnO (22.2 m²/g)[3], Fe^x@CS (18.0 m²/g) and Fe⁰/Fe₃C@CS (42.3 m²/g)[9]. The existence of porous structure can significantly improve the interfacial polarization effect, which can further enhance the dielectric loss in the high frequency range, thus affecting the EMW absorption performance of the nanocomposites.

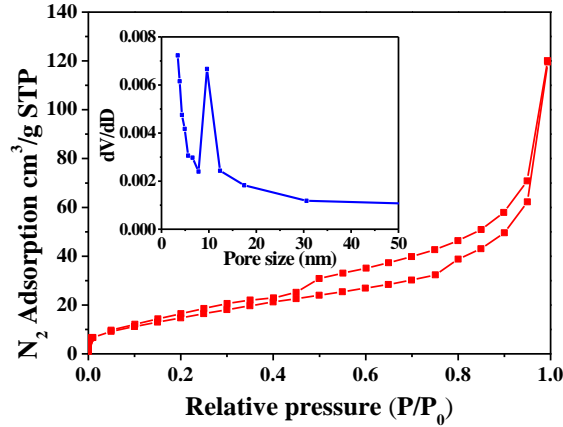


Fig. 1 Nitrogen sorption isotherm and pore size distribution of core/shell Fe@CNCs.

3.1. Total solid and Fe@CNCs yield

To better define the yield of the product, in this work, the total solid is the weight of the raw product in each batch and the Fe@CNCs yield is defined as the mass ratio of the raw product after and before acid washing treatment. Fig. 2a shows the total solid under different microwave power. It increases first and then decreases with the increase of microwave power, and the maximum value reaches 200 mg at 1800 W. Previous studies have shown that the higher the microwave power, the more intense the MW-M discharge[32], which contributes to the decomposition of organometallic compounds and the carbonization of amorphous carbon. However, when the microwave power is too high, violent discharges will lead to the evaporation of raw materials. At this point, the greater the power, the faster the evaporation, resulting in a decline in yield. The variation regularity of total solid under different microwave irradiation time was shown in Fig. 2b, that the weight increases first with the increase of microwave irradiation time, and it tends to be stable after 4 min. This is because a relatively short irradiation time cannot provide sufficient energy for the carbonization process and a large amount of ferrocene was carried by the evaporated solution.

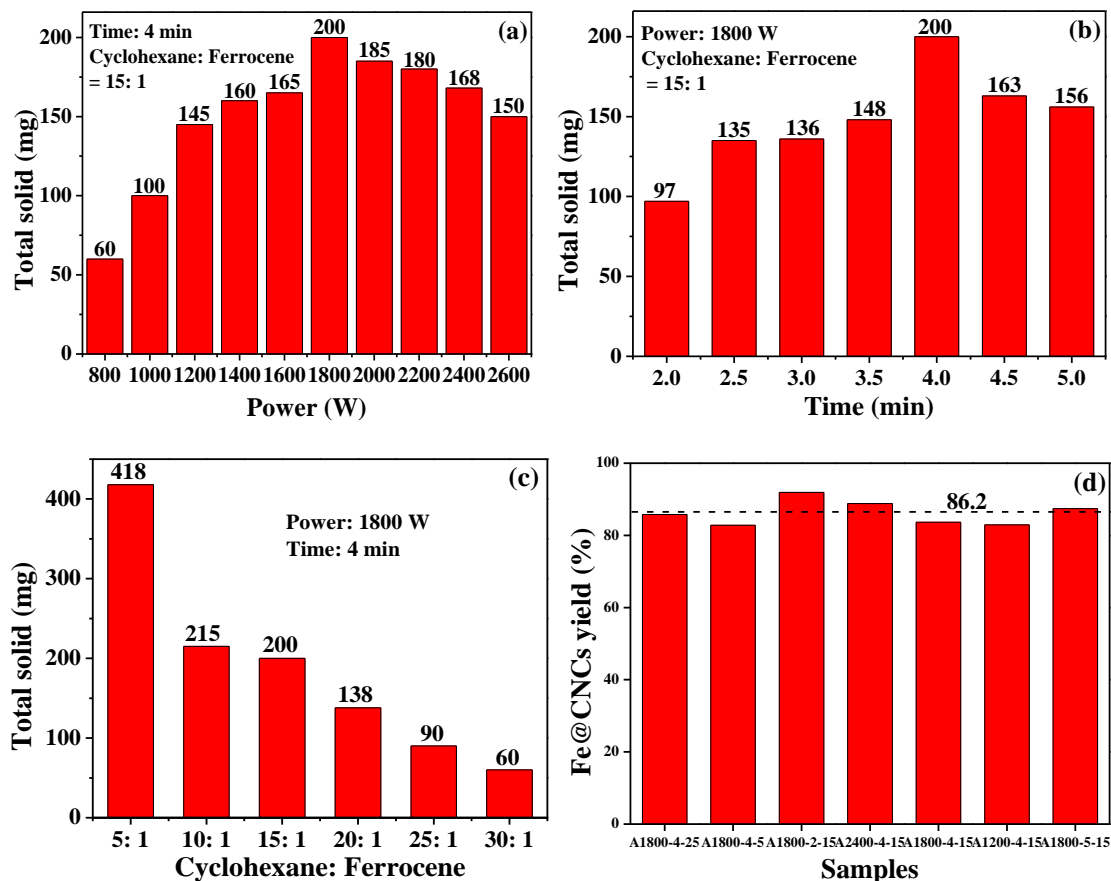


Fig. 2 Total solid (a, b and c) of the raw product in each batch under different working conditions and Fe@CNCs yield (d).

Fig. 2c shows that the total solid is positively correlated with the content of ferrocene in the raw material, which means that the total solid is mainly determined by the ferrocene content. It is known that the addition amount of ferrocene of the six samples is 1.8, 0.9, 0.6, 0.45, 0.36 and 0.3 g, the mass ratio of total solid/ferrocene can be calculated as 0.23, 0.24, 0.33, 0.31, 0.25 and 0.20, respectively. It can be seen that the amount of nano-carbon particles formed as a fraction of the absolute amount of ferrocene used remains relatively constant or appears to be irrespective of the concentration of ferrocene in cyclohexane, suggesting that ferrocene, as opposed to the solvent of cyclohexane used, is primarily responsible for the formation and deposition of the nano-carbon particles. Indeed, it was found that most of the cyclohexane can be

condensed out and recycled in the downstream process. The yields of nanocarbon particles were calculated to be more than 20%, which is significantly higher than those of other methods, such as microwave arcing process (~15%)[14] and explosive method (10-15%)[26]. In addition, all carbon particles showed similar content of Fe@CNCs, which was averaged at 86.2 % (as shown in Fig. 2d), confirming the exceedingly high efficiency of the formation of the ferromagnetic encapsulated nanoparticles. Compared with the carbon arc discharge (8-25%)[38], the Fe@CNCs yield obtained by this methodology has obvious advantages, indicating a high process efficiency. Both high yield and short preparation cycle have laid a solid foundation for the efficient application of MW-M discharge. Based on the above data, the formation mechanism of Fe@CNCs can be speculated. That is, hot-spot effect and plasma effect generated by MW-M discharge induce the micro-discharge of Fe in the ferrocene, which causes the collapse of cyclopentadiene on both sides of the Fe atom. Due to the desirable environmental conditions and the catalytic effect of iron[39-41], cyclopentadiene coated around the Fe atom can be thoroughly dehydrogenated and carbonized and eventually lead to the formation of the integrated graphite-like structures.

3.2. Phase and structure characterization

Fig. 3 shows the XRD patterns of seven samples in Fig. 2d. It can be seen that all samples are highly characterized by the characteristic presence of highly graphitized nanocarbon structures (002), body centered cubic (bcc) iron (α -Fe) and cementite iron carbide (Fe_3C), with the iron core consists of mainly α -Fe and some quantities of Fe_3C . This suggests that the prepared iron-cored CNCs via the microwave-metal discharge all

have highly ordered graphite layers with well-regulated iron as the core. The results shown by Fig. 3 also indicate that the crystalline phase composition of the Fe@CNCs samples prepared did not appear to be affected by the microwave power, irradiation time and the ratio of precursor materials.

It was found from Fig. 3 that the diffraction peaks for the Fe phase present in the core of the Fe@CNCs are consistent with the standard phase (110), (200) and (220) of pure α -Fe, with the intensity of α -Fe diffraction peak being the strongest when the microwave power is 1800 W and the irradiation time is 4-5 min. A further increase in power output levels and duration times was found to lead to decreased intensity of both graphitized carbon and α -Fe diffraction peaks, presumably due to the enhanced evaporation loss of both the precursor feedstocks and potentially the carbon and/or iron species formed. This suggests that there exist optimal operational conditions to allow the development of desirable Fe@CNCs the iron core of samples. XRD is ideally suitable for investigating the evolution of graphitic structure of the nanoparticles. The diffraction patterns of the samples with different cyclohexane/ferrocene ratios were shown in Fig. S1. According to Mering-Maire equation (Eq.1) shown below [42], the degree of graphitization was calculated to be 57.4% (A1800-4-25), 69.3% (A1800-4-15) and 60.7% (A1800-4-5), respectively.

$$g = \frac{0.3440 - d_{002}}{0.3440 - 0.3354} \times 100\% \quad (1)$$

Where g is the graphitization degree, d_{002} is the interlayer spacing along the c axis of graphite.

The results intuitively show that the graphitization degree of the iron-cored nanocarbon

particles can reach up to about 70%. The sample prepared from using a cyclohexane/ferrocene ratio of 15 (A1800-4-15) has a higher graphitization degree, followed by the sample A1800-4-5. This suggests that the amount of ferrocene available is vital for the formation of the well-graphited carbon shells. In addition, it is noteworthy that the presence of cementite Fe_3C , which was detected in appreciable quantities, may suggest that this compound may serve as an intermediate for the formation of the graphite layers[39, 43]. Since Fe_3C usually can only be formed at extremely high temperatures, this highlights the capability of microwave-metal discharge in creating the desirable localized high temperatures and associated pressures for the formation of quality metal-cored nanocarbon particles.

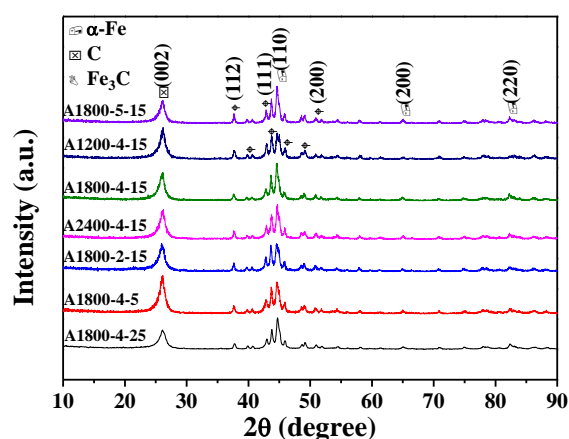


Fig. 3 XRD patterns of different core/shell Fe@CNCs

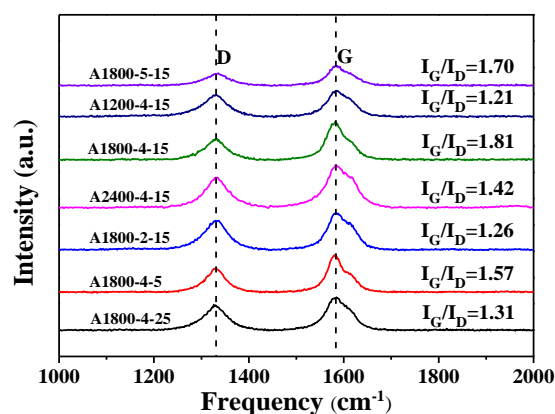


Fig. 4 Raman spectra of different core/shell Fe@CNCs.

To further characterize the degree of graphitization of the metal-cored nanocarbon particles, which is an important factor that determines the quality of the materials for advanced applications (e.g. as an EMW absorbing material[44]), Raman spectroscopy was used to reveal further information. Fig. 4 shows the Raman spectra of the Fe@CNCs prepared under different conditions. All the samples present two typical characteristic peaks, which are often respectively referred to as the D band (1333 cm^{-1}) that is related to the disorder of the carbon material and the G band (1586 cm^{-1}) that is used to indicate the crystalline degree of the hexagonal lattices of carbon materials[45]. As a result, the intensity ratio of G and D band (I_G/I_D) is often used to characterize the graphitization degree of the carbon material, with samples having a higher graphitization degree giving rise to greater I_G/I_D of the ratio[38]. The Raman results show that the I_G/I_D value of all the samples is significantly higher than 1.2 and with the sample prepared with a microwave power output level of 1800W and irradiation time of 4 min having the highest I_G/I_D ratio of 1.81, which are significantly higher than those of the metal-cored CNCs prepared from using other methodologies, such as high-temperature carbonization[44], carbon arc discharge[38] and thermal plasma torch method[46].

It is well known that iron core has catalytic effect on the formation and growth of graphitized nanocarbon shells[39], but clearly the catalytic activity of iron alone cannot fully account for the significantly higher degree of graphitization obtained for the Fe@CNCs prepared from using the microwave-metal discharge methodology. It can be seen that for a given duration time of microwave discharge, the graphitization degree

of Fe@CNCs first increased with increasing the power output up to 1800W, followed by a decrease with a further increase in the output level used. It is believed that the excessive power output may lead to excessive rate of carbon formation and thus affect the crystallization or alignment of the carbon on the surface of the iron core, giving rise to greater defects of the carbon shells formed. Similar trend was also observed with respect to the effect of microwave-metal discharge time (e.g. Sample A1800-2-15, A1800-4-15 and A1800-5-15). For a given power output level, it was found that the use of longer irradiation time led to the formation of larger sizes of Fe-cored nanocarbon capsules but at a cost of reduced degree of graphitization, due to the entrapment of amorphous carbon in the capsule structures during the process of particle deposition or agglomeration.

Fig. 5 shows the SEM and TEM images of the four selected samples. It is evident that all the nanocapsules samples prepared are essentially spherical nanoparticles or their clusters containing a typical core-shell structure, with nanocarbon tubes also observed in appreciable quantities, due to the catalytic effect of metallic iron[47] and the high temperatures induced by the MV discharges. The sizes of the nano-capsules or their clusters vary typically from 30 to 100 nm. The occurrence of nano-capsule clusters or agglomerates is clearly attributable to the strong cohesion or even electromagnetic interaction between the Fe-cored CNCs of nanoparticles as to be discussed later.

The TEM image (see Fig. 5b) reveals that the carbon shell of Fe-cored nano-capsules has a distinctive layered structure with an interval spacing of around ~ 0.34 nm, which is very close to the theoretical layer spacing of the graphite (0.3354), highlighting the

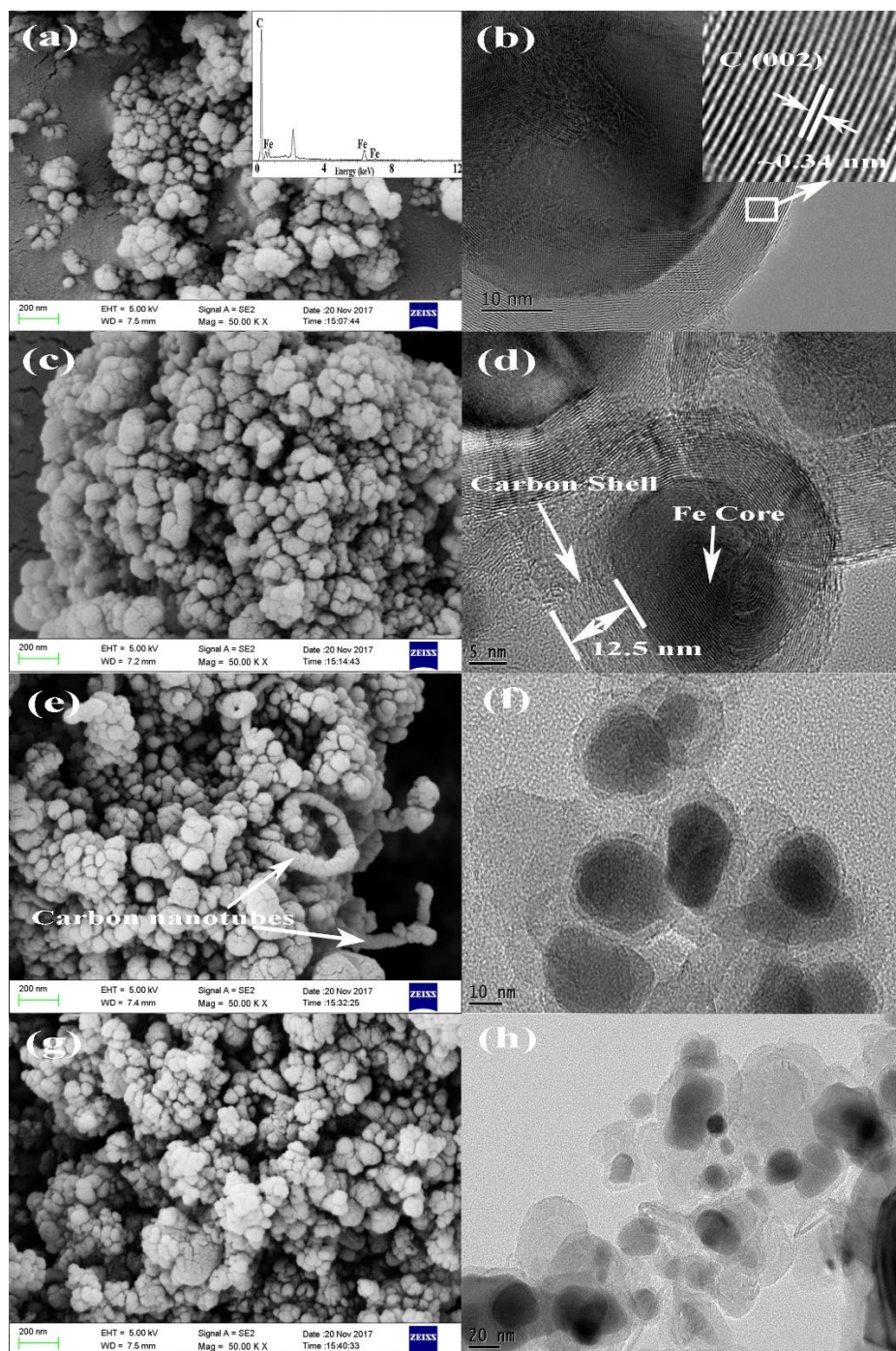


Fig. 5 SEM (a, c, e and g) and TEM (b, d, f and h) images of core/shell Fe@CNCs, A1800-4-5 (a, b), A1800-2-15 (c, d), A2400-4-15 (e, f) and A1800-4-15 (g, h), inset in SEM image (a) is the corresponding EDS spectrum.

high degree of graphitization of the carbon shells. Additionally, the thickness of the crystalline carbon shell was obtained to be more than 10 nm (as shown in Fig. 5b and Fig. 5d), which is higher than virtually all previous reported metal-cored carbon

capsules prepared by high temperature carbonization, arc discharge and explosion methods[21, 48, 49]. It is also evident from the SEM/TEM images that the Fe metal particles are well seeded into the core of the carbon lattice with no evident structural defects, highlighting the novel material integrity and potential super stability of the Fe-cored nanoparticles even in hostile thermo-oxidative environments. High integrity of the carbon shell plays a decisive role in securing a long lifetime performance in different application environment. For instance, the disintegration or even rupture of the carbon shell[50] will lead to the corrosion or eradication of the metal core, transforming the metal-cored nanocapsules into hollow onion-like structures. The superior integrity of the carbon shell of the metal-cored nanocapsules augurs extremely well for the lasting lifetime performance of these materials in various environments, highlighting the capability of MW-M discharge in fabricating superior metal-cored carbon capsules. However, in this work, the onion-like carbon shell was rarely found, indicating that the shell of Fe@CNCs prepared by MW-M discharge have a high integrity.

3.3 TGA characterization and thermo-oxidative stability of Fe@CNCs

Thermal gravimetric analysis (TGA) was used to examine the relative composition and the thermo-oxidative stability of the Fe@CNCs capsules prepared under different conditions[51]. Fig. 6 shows the proximate analyses for the Fe@CNCs samples. As can be seen, the iron content in the form of iron oxides varied from 17.5 wt% to 22.0 wt%, with those prepared at higher MW output levels and longer discharge times generally having higher iron or lower carbon contents. The material balance of iron from the preparation can be expressed as follows: Iron in ferrocene = Iron removed by acid-

washing + Iron coated in carbon shells + Iron loss. Based on the mass conservation law, the effective utilization rate of iron in this preparation was calculated to be between 20-25% at a power level of 1800 W and an irradiation time of 4 mins. However, it is interesting to note that the sample prepared at the highest ferrocene concentration (sample A1800-4-5) was found to have the lowest iron (17.5 wt%) or highest carbon content (82.5 wt%), and this may suggest that the carbon contained in the ferrocene is preferentially deposited out at a loss of iron or some of the ferrocene-contained iron is not encapsulated to form the iron-cored nanocarbon capsules. By and large, the proximate analyses show that a cyclohexane/ferrocene mass ratio of 15 appears to be the optimal for the efficient formation of the Fe-cored capsules. Compared to other carbon-coated nanocapsules prepared from using other methodologies[5, 52], the carbon contents or the thicknesses of the carbon shells of the Fe-cored capsules generated from the MW-M discharge are considerably higher, highlighting again the novel capability of MW discharge in fabricating high quality of metal-core capsules.

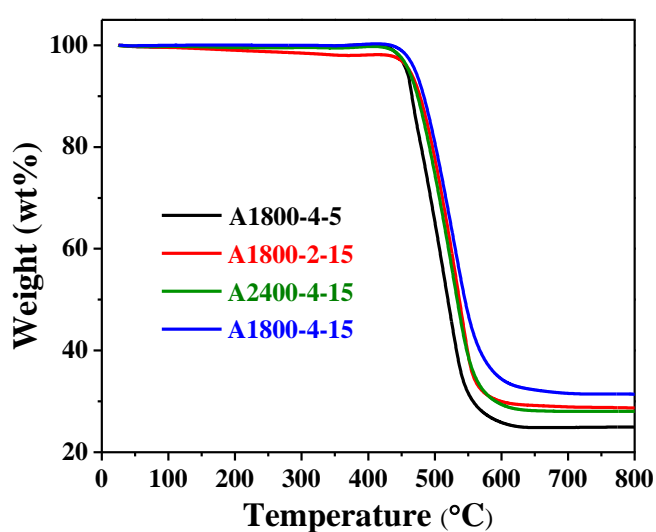


Fig. 6 TGA curves of different core/shell Fe@CNCs in air with a heating rate of 10 °C/min, the Fe content of the sample A1800-4-5, A1800-2-15, A2400-4-15 and A1800-4-15 are calculated to be 17.5, 20.1, 19.6 and 22.0 wt%, respectively.

In order to investigate the anti-corrosion performance and thermo-oxidative stability of the Fe-cored nanocapsules, the sample A1800-4-5 was first subjected to an acid washing treatment in dilute nitric acid under ambient and vigorous stirring conditions for variable duration times, before they are subjected to the burn-out tests in air with TGA, which were used as an accelerated testing of the thermo-oxidative stability of the capsule samples. Fig. 7 shows the accelerated thermo-oxidative stability testing results of the samples before and after the acid treatments. The slight weight gain observed at temperatures up to 420 °C for the sample A1800-4-5 before the acid treatment are believed to result from the oxidation of trace quantities of free or partly encapsulated iron^[9] whereas the following slight weight loss obtained from 420 to 450 °C was due to the burnout of the amorphous carbons formed, respectively. This confirms that the formation of amorphous carbon and non or partly encapsulated iron appears to be closely related, and this phenomenon seems to occur mainly at high ferrocene concentrations used under the MW-M discharge conditions.

In general, the TGA results indicate that all Fe-cored capsules demonstrate exceedingly high thermo-oxidative stability at temperatures up to 420 °C and no evident effect of the strongly aggressive acid treatment was observed on the stability. This highlights the robust anti-corrosion performance and novel thermo-oxidative stability of Fe@CNCs prepared via the MW discharge methodology, which are significantly higher than those fabricated with other methodologies, such as hydrothermal, arc-discharge and CVD method[14, 53], where the Fe or other metal-cored capsules can only afford temperatures generally well below 240 °C.

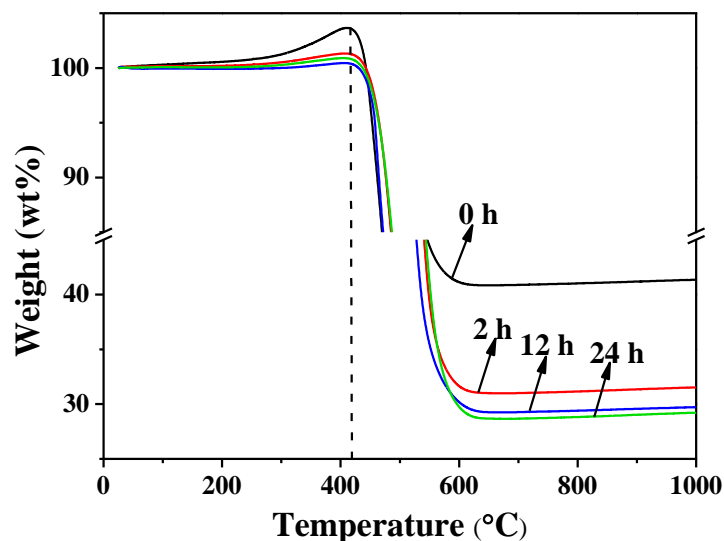


Fig. 7 TGA curves of sample A1800-4-5 after different time acid-washing, carried out in air with a heating rate of 10 °C/min.

To further investigate the thermos-oxidative stability of the Fe-cored nanocapsules prepared, the sample A1800-4-5 was selected for an annealing treatment in air for 2 h at a pressure of -0.05 MPa and temperature of 550 °C. Fig. 8a shows the Raman spectra for the A1800-4-5 sample before and after the annealing treatment. It can be seen that the I_G/I_D value of the sample after the annealing treatment decreased from 1.57 to 1.25, but it is still considerably higher than most of the other Fe@CNCs reported with other methodologies[11, 14], being indicative of the novel integrity of the Fe/carbon shell structures. The XRD pattern for the annealed sample (Fig. 8b) shows that the Fe_3C species present in the capsule structures have been transformed into Fe_3O_4 after the annealing treatment. Compared with the CNCs with Fe/ Fe_3C as the core, the capsules with Fe/ Fe_3O_4 -cored exhibit better electrochemical performance. More importantly, the detection of crystal lattice of Fe_3O_4 as can be clearly seen from the inset in Fig. 8b indicates that the thermal annealing treatment contributes to the further development of the desirable crystalline structures, which helps to enhance the metal-cored capsules'

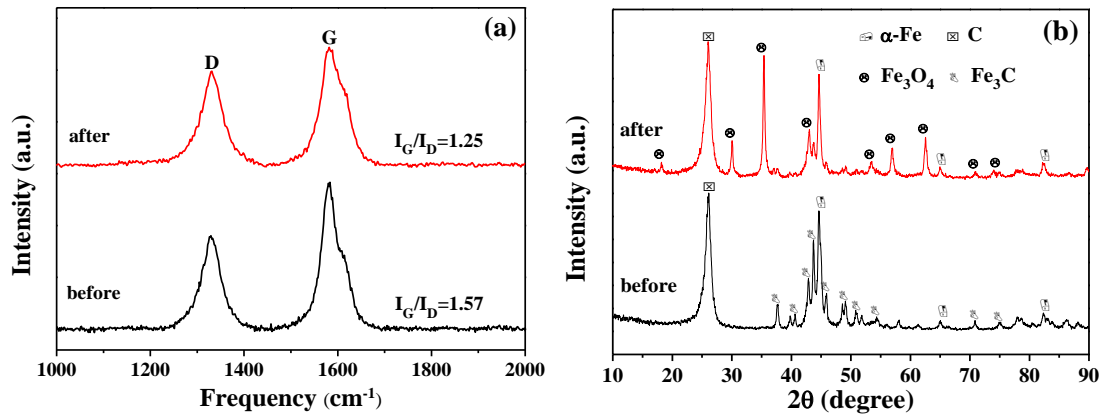


Fig. 8 Raman spectra (a) and XRD patterns (b) of core/shell Fe@CNCs before and after thermal annealing in air.

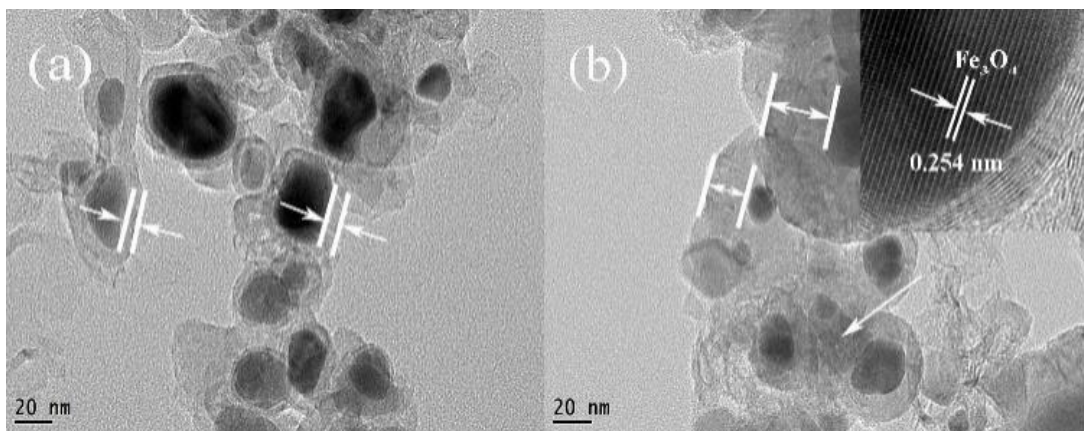


Fig. 9 High resolution TEM images of core/shell Fe@CNCs before (a) and after (b) thermal annealing in air.

saturation magnetization[54]. It is worth mentioning that the chemical composition of the residual solids remains the same i.e. C, α -Fe and Fe₃C after thermal degradation in N₂ atmosphere. The high resolution TEM images shown in Fig. 9 show that after the thermal annealing treatment, the size and carbon layer thickness of the capsule samples increased significantly, indicating a better anti-corrosion performance. It was also found from the TEM images that the degree of structural disorder and fusion between the small nanoparticles is increased (Fig. 9b), which is consistent with the observed decrease in the I_G/I_D value shown in Raman spectrum in Fig. 8a. It is noteworthy that a remarkable recovery of higher than 95% was achieved from the nitric acid washing of

the thermally annealed sample, being suggestive of the novel thermo-oxidative stability of the Fe@CNCs in extreme environments, for example, as stealth material on the surface of high speed flying objects[55].

3.4. Performance assessment of the Fe-cored nanocapsules prepared as magnetic and EMW absorbing materials

The magnetic hysteresis loop obtained from a magnetometer at room temperature, as shown in Fig. 10, is used to characterize the magnetic absorption characteristics of the synthesized nanocapsules. It can be seen that the Fe-cored nanocapsules exhibit strong ferromagnetic behavior and the magnetization reaches saturation at 10 kOe. The saturation magnetization (M_S) value of the sample is 23.1 emu g⁻¹, which is equivalent approximately to 11% of the bulk iron contained[56]. It is known that the M_S of the Fe@CNCs is mainly determined by the total Fe content[38], so the value can be further improved by increasing the amount of encapsulated iron content in the structure. Based on this, it can be determined that the sample A1800-4-15 will exhibit better magnetic performance than the sample A1800-4-5 because of its higher iron content.

It is also interesting to note that the Fe@CNC capsules show extraordinary magnetic properties as demonstrated in a simple experiment where it was found that all the Fe@CNCs particles dispersed in an aqueous suspension can be quickly separated from the mixture by using a common magnet, changing the colour of the aqueous suspension from black to colorless as shown in the inset of Fig. 10. In particular, the advantage of easy separation of the products is unattainable by CVD method, and it can be used as recyclable catalyst for chemical reactions enhancement.

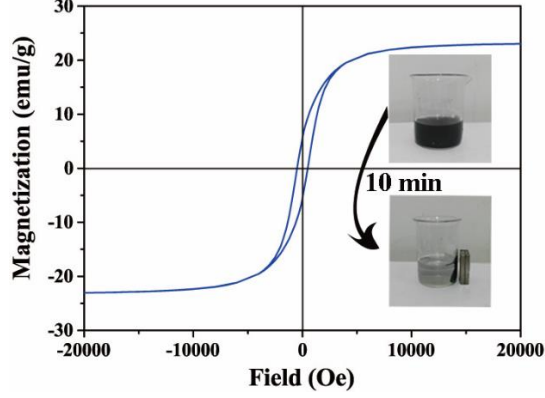


Fig. 10 Magnetic hysteresis loop of core/shell Fe@CNCs, take sample A1800-4-5 as an example.

It is known that the EMW absorption performance is mainly determined by the dielectric tangent loss ($\tan \delta_e = \varepsilon'' / \varepsilon'$) and the magnetic tangent loss ($\tan \delta_m = \mu'' / \mu'$), as shown in Fig. 11. Among them, ε' , ε'' , μ' and μ'' are the real and imaginary part of complex permittivity and complex permeability, respectively. It should be noted that the drastic fluctuations of these two curves are caused by the relaxation process[29]. For instance, the $\tan \delta_m$ is always smaller than the $\tan \delta_e$ in the frequency range from 2 to 18 GHz, and the $\tan \delta_m$ changes slightly around zero. Compared with other nanocapsules[11, 21], the material has a high dielectric loss, which can improve not only the conductivity of the material but also the attenuation constant. In order to have an explicit understanding of the EMW absorption performance of the Fe-cored nanocapsules, the reflection loss (RL) was calculated via testing complex permeability and permittivity at different frequency based on the transmission line theory as follows[31, 57]:

$$R_L(dB) = 20 \log \left| \frac{Z_{in} - Z_0}{Z_{in} + Z_0} \right| \quad (2)$$

$$Z_{in} = Z_0 \sqrt{\frac{\mu_r}{\varepsilon_r}} \tanh \left[j \left(\frac{2\pi f d}{c} \right) \sqrt{\varepsilon_r \mu_r} \right] \quad (3)$$

Where Z_0 is the input impedance of free space (usually Z_0 get 1), Z_{in} is the input

impedance of the absorber, ϵ_r and μ_r are the complex permittivity and complex permeability, respectively, f is the frequency of the EMW, c is the light velocity in the free space and d is the thickness of the absorber.

Fig. 12 shows the RL values of the prepared Fe@CNCs, and it can be seen that the thickness of the packed absorber varies from 1.0 mm to 5.0 mm. When the RL values is higher than -10 dB, it means that more than 90% of the EMW will be absorbed and when this value is decreased to -20 dB, the absorption ratio can reach 99%. It is clear that the sample exhibits a great EMW absorption performance and with the RL value being close to as low as -22.5 dB at 10.2 GHz for a thickness of 2.5 mm. The minimal RL values of the sample are less than -18 dB for a thickness of 1.5-5 mm, which is even smaller than that of graphene (-11 dB)[37]. This indicates that the material has a better EMW absorption performance than pure graphite. It is interesting that the strongest RL value was found to be in the favourable high frequency region, and this compares to typical magnetic metal materials which their absorptive properties are only observed in the low frequency region. This is due to the high resistivity of the graphite shell, which can effectively reduce the effect of the eddy currents on the magnetic loss at high frequency[29, 58]. In addition, as shown in the figure, with the RL values being less than -10 dB, the corresponding absorption bandwidth can reach up to 13.8 GHz (4.2-18 GHz). Compared with other core-shell nanocomposites such as CoNi@SiO₂@TiO₂[59], Co_xFe_y@C[60], (Fe, Ni)/C NPs^[4] and (Fe)C NPs^[30], the Fe@CNCs prepared from using MW discharge display desirable absorption behavior over a significantly wider range of EMW bandwidth. It is also found that for a RL value being as low as -10 dB,

the matching thickness is only 1.5 mm, which is significantly thinner than the reported thickness for other materials, which ranged mostly from 2 to 4 mm[3, 21, 61]. The results suggest that to achieve the same level of EMW absorption, the required coating thickness of Fe@CNCs will be much thinner than those of the aforementioned other metal-cored nanocomposites. Calculations also demonstrate that the added weight of Fe@CNCs in the absorber is only 30 wt%, which is also significantly lower than those of other previously reported materials, which are usually more than 40 wt% [21]. Based on the above data, it is believed that the Fe@CNCs prepared from microwave discharge is a super EMW absorbing material over a wide-range of bandwidth, outperforming virtually all the previously reported materials prepared from using other approaches.

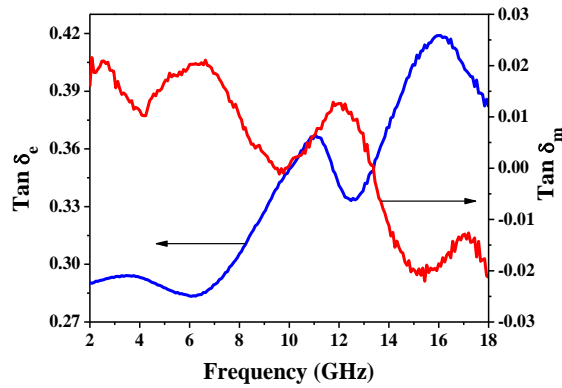


Fig. 11 Dielectric tangent loss ($\tan \delta_e$) and magnetic tangent loss ($\tan \delta_m$) of core/shell Fe@CNCs in 2-18 GHz.

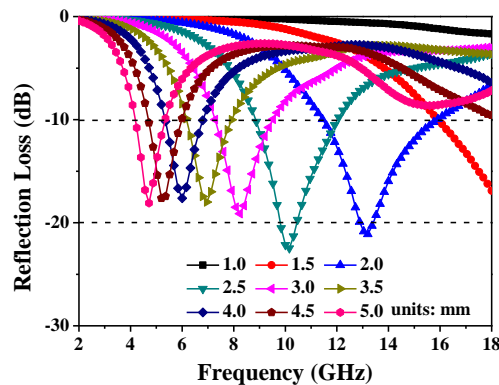


Fig. 12 Reflection loss of core-shell Fe@CNCs with absorber thickness of 1-5 mm.

4. Conclusions

The use of MW-M discharge as novel facile technology for the fast production of high purity Fe@CNCs has been explored with great promise. Using ferrocene dissolved in cyclohexane as the precursor material, the results demonstrate that Fe-cored nanocarbon capsules with exceedingly high material integrity were generated, with the highly graphitized carbon shells being almost exclusively derived from the precursor ferrocene, giving rise to the virtually full recovery of the solvent of cyclohexane used, and this highlights the novel capability of MW-M discharge in selectively targeting the ferrocene precursor material for the formation of F@CNCs particles. It was also found that the Fe-cored nanocapsules have super anti-corrosion performance and novel thermo-oxidative stability, outperforming virtually all previously reported M@CNCs prepared from using other methodologies. Thermal annealing treatment in air was found to lead to the desirable transformation of Fe_3C to Fe_3O_4 , which further helps to improve the electrochemical properties of the material. EMW absorption tests reveal that with a thin layer of the carbon shells having extraordinary anti-corrosion and thermos-oxidative stability, the Fe@CNCs particles show exceedingly high absorption of EMW across a wide-range of EMW bandwidth. The results from the exploratory investigation, which appears to be the first of its kind to the best of our knowledge, augurs extremely well for the use of MW-M discharge as a novel approach for synthesizing novel functionalized materials for targeted applications such as the EMW absorbing materials, high-performance electrode materials and easy-to-separate catalysts.

Acknowledgements

This work was supported by the National Natural Science Foundation of China (Grant 51506116, Grant 51576118 and Grant 51376112), Shandong Science Fund for Distinguished Young Scholars (JQ201514), Major Research Project of Shandong Science Fund(ZR2017ZC0734) and the Young Scholars Program of Shandong University (2016WLJH37).

References

- [1] Lukanov P, Anuganti VK, Krupskaya Y, Galibert A-M, Soula B, Tilmaciu C, et al. CCVD Synthesis of Carbon-Encapsulated Cobalt Nanoparticles for Biomedical Applications. *Advanced Functional Materials*. 2011;21(18):3583-8.
- [2] Zhang X, Liu Z. Recent advances in microwave initiated synthesis of nanocarbon materials. *Nanoscale*. 2012;4(3):707-14.
- [3] Sun D, Zou Q, Wang Y, Wang Y, Jiang W, Li F. Controllable synthesis of porous Fe₃O₄@ZnO sphere decorated graphene for extraordinary electromagnetic wave absorption. *Nanoscale*. 2014;6(12):6557-62.
- [4] Liu XG, Li B, Geng DY, Cui WB, Yang F, Xie ZG, et al. (Fe, Ni)/C nanocapsules for electromagnetic-wave-absorber in the whole Ku-band. *Carbon*. 2009;47(2):470-4.
- [5] Ding D, Wang Y, Li X, Qiang R, Xu P, Chu W, et al. Rational design of core-shell Co@C microspheres for high-performance microwave absorption. *Carbon*. 2017;111:722-32.
- [6] Kovalenko I, Bucknall DG, Yushin G. Detonation Nanodiamond and Onion-Like-Carbon-Embedded Polyaniline for Supercapacitors. *Advanced Functional Materials*. 2010;20(22):3979-86.
- [7] Galeano C, Baldizzone C, Bongard H, Spliethoff B, Weidenthaler C, Meier JC, et al. Carbon-Based Yolk-Shell Materials for Fuel Cell Applications. *Advanced Functional Materials*. 2014;24(2):220-32.
- [8] Chen M, He Y, Wang X, Hu Y. Complementary enhanced solar thermal conversion performance of core-shell nanoparticles. *Applied Energy*. 2018;211:735-42.
- [9] Wang Y, Sun H, Duan X, Ang HM, Tadé MO, Wang S. A new magnetic nano zero-valent iron encapsulated in carbon spheres for oxidative degradation of phenol. *Applied Catalysis B: Environmental*. 2015;172-173:73-81.
- [10] Kainz QM, Linhardt R, Grass RN, Vilé G, Pérez-Ramírez J, Stark WJ, et al. Palladium Nanoparticles Supported on Magnetic Carbon-Coated Cobalt Nanobeads: Highly Active and Recyclable Catalysts for Alkene Hydrogenation. *Advanced Functional Materials*. 2014;24(14):2020-7.
- [11] Zhang Y, Huang Y, Chen H, Huang Z, Yang Y, Xiao P, et al. Composition and structure control of ultralight graphene foam for high-performance microwave absorption. *Carbon*. 2016;105:438-47.
- [12] Zhou H, Wang J, Zhuang J, Liu Q. A covalent route for efficient surface modification of ordered mesoporous carbon as high performance microwave absorbers. *Nanoscale*. 2013;5(24):12502-11.
- [13] Schwenke AM, Hoepfener S, Schubert US. Synthesis and Modification of Carbon Nanomaterials

utilizing Microwave Heating. *Adv Mater.* 2015;27(28):4113-41.

[14] Hsin YL, Lin CF, Liang YC, Hwang KC, Horng JC, Ho JaA, et al. Microwave Arcing Induced Formation and Growth Mechanisms of Core/Shell Metal/Carbon Nanoparticles in Organic Solutions. *Advanced Functional Materials.* 2008;18(14):2048-56.

[15] Borysiuk J, Grabias A, Szczytko J, Bystrzejewski M, Twardowski A, Lange H. Structure and magnetic properties of carbon encapsulated Fe nanoparticles obtained by arc plasma and combustion synthesis. *Carbon.* 2008;46(13):1693-701.

[16] Chen Y-j, Xiao G, Wang T-S, Ouyang Q-Y, Qi L-H, Ma Y, et al. Porous Fe₃O₄/Carbon Core/Shell Nanorods: Synthesis and Electromagnetic Properties. *The Journal of Physical Chemistry C.* 2011;115(28):13603-8.

[17] Ozaki J, Kimura N, Anahara T, Oya A. Preparation and oxygen reduction activity of BN-doped carbons. *Carbon.* 2007;45(9):1847-53.

[18] Zhou Z, Liu R. Fe₃O₄@polydopamine and derived Fe₃O₄@carbon core-shell nanoparticles: Comparison in adsorption for cationic and anionic dyes. *Colloids and Surfaces A: Physicochemical and Engineering Aspects.* 2017;522:260-5.

[19] Zhang XF, Dong XL, Huang H, Lv B, Zhu XG, Lei JP, et al. Synthesis, growth mechanism and magnetic properties of SiO₂-coated Co nanocapsules. *Acta Materialia.* 2007;55(11):3727-33.

[20] Liu X, Sun Y, Feng C, Jin C, Li W. Synthesis, magnetic and electromagnetic properties of Al₂O₃/Fe oxides composite-coated polyhedral Fe core-shell nanoparticles. *Applied Surface Science.* 2013;280:132-7.

[21] Wu N, Liu X, Zhao C, Cui C, Xia A. Effects of particle size on the magnetic and microwave absorption properties of carbon-coated nickel nanocapsules. *Journal of Alloys and Compounds.* 2016;656:628-34.

[22] Han D, Or SW, Dong X, Liu B. FeSn₂/defective onion-like carbon core-shell structured nanocapsules for high-frequency microwave absorption. *Journal of Alloys and Compounds.* 2017;695:2605-11.

[23] Lu B, Dong XL, Huang H, Zhang XF, Zhu XG, Lei JP, et al. Microwave absorption properties of the core/shell-type iron and nickel nanoparticles. *Journal of Magnetism and Magnetic Materials.* 2008;320(6):1106-11.

[24] Qiu J, Li Y, Wang Y, An Y, Zhao Z, Zhou Y, et al. Preparation of carbon-coated magnetic iron nanoparticles from composite rods made from coal and iron powders. *Fuel Processing Technology.* 2004;86(3):267-74.

[25] Sergiienko R, Shibata E, Akase Z, Suwa H, Nakamura T, Shindo D. Carbon encapsulated iron carbide nanoparticles synthesized in ethanol by an electric plasma discharge in an ultrasonic cavitation field. *Materials Chemistry and Physics.* 2006;98(1):34-8.

[26] Luo N, Li X, Wang X, Yan H, Zhang C, Wang H. Synthesis and characterization of carbon-encapsulated iron/iron carbide nanoparticles by a detonation method. *Carbon.* 2010;48(13):3858-63.

[27] Zhang N, Liu S, Fu X, Xu Y-J. Synthesis of M@TiO₂ (M = Au, Pd, Pt) Core-Shell Nanocomposites with Tunable Photoreactivity. *The Journal of Physical Chemistry C.* 2011;115(18):9136-45.

[28] Chen Y, Song B, Li M, Lu L, Xue J. Fe₃O₄ Nanoparticles Embedded in Uniform Mesoporous Carbon Spheres for Superior High-Rate Battery Applications. *Advanced Functional Materials.* 2014;24(3):319-26.

[29] Liu XG, Ou ZQ, Geng DY, Han Z, Jiang JJ, Liu W, et al. Influence of a graphite shell on the thermal and electromagnetic characteristics of FeNi nanoparticles. *Carbon.* 2010;48(3):891-7.

- [30] Zhang XF, Dong XL, Huang H, Lv B, Lei JP, Choi CJ. Microstructure and microwave absorption properties of carbon-coated iron nanocapsules. *Journal of Physics D: Applied Physics*. 2007;40(17):5383-7.
- [31] Shah A, Wang Y, Huang H, Zhang L, Wang D, Zhou L, et al. Microwave absorption and flexural properties of Fe nanoparticle/carbon fiber/epoxy resin composite plates. *Composite Structures*. 2015;131:1132-41.
- [32] Sun J, Wang W, Yue Q, Ma C, Zhang J, Zhao X, et al. Review on microwave–metal discharges and their applications in energy and industrial processes. *Applied Energy*. 2016;175:141-57.
- [33] Wang W, Liu Z, Sun J, Ma Q, Ma C, Zhang Y. Experimental study on the heating effects of microwave discharge caused by metals. *AIChE Journal*. 2012;58(12):3852-7.
- [34] Sun J, Wang Q, Wang W, Song Z, Zhao X, Mao Y, et al. Novel treatment of a biomass tar model compound via microwave-metal discharges. *Fuel*. 2017;207:121-5.
- [35] Wang W, Wang B, Sun J, Mao Y, Zhao X, Song Z. Numerical simulation of hot-spot effects in microwave heating due to the existence of strong microwave-absorbing media. *Rsc Advances*. 2016;6(58):52974-81.
- [36] Bajpai R, Wagner HD. Fast growth of carbon nanotubes using a microwave oven. *Carbon*. 2015;82:327-36.
- [37] Ren YL, Wu HY, Lu MM, Chen YJ, Zhu CL, Gao P, et al. Quaternary nanocomposites consisting of graphene, Fe₃O₄@Fe core@shell, and ZnO nanoparticles: synthesis and excellent electromagnetic absorption properties. *ACS applied materials & interfaces*. 2012;4(12):6436-42.
- [38] Bystrzejewski M, Łabędź O, Kaszuwara W, Huczko A, Lange H. Controlling the diameter and magnetic properties of carbon-encapsulated iron nanoparticles produced by carbon arc discharge. *Powder Technology*. 2013;246:7-15.
- [39] Schaper AK, Hou HQ, Greiner A, Phillipp F. The role of iron carbide in multiwalled carbon nanotube growth. *Journal of Catalysis*. 2004;222(1):250-4.
- [40] Bauman YI, Kutaev NV, Plyusnin PE, Mishakov IV, Shubin YV, Vedyagin AA, et al. Catalytic behavior of bimetallic Ni–Fe systems in the decomposition of 1,2-dichloroethane. Effect of iron doping and preparation route. *Reaction Kinetics, Mechanisms and Catalysis*. 2017;121(2):413-23.
- [41] Lee JY, Kim NY, Shin DY, Park H-Y, Lee S-S, Joon Kwon S, et al. Nitrogen-doped graphene-wrapped iron nanofragments for high-performance oxygen reduction electrocatalysts. *Journal of Nanoparticle Research*. 2017;19(3).
- [42] Heckmann A, Fromm O, Rodehorst U, Münster P, Winter M, Placke T. New insights into electrochemical anion intercalation into carbonaceous materials for dual-ion batteries: Impact of the graphitization degree. *Carbon*. 2018;131:201-12.
- [43] Fedoseeva YV, Bulusheva LG, Okotrub AV, Vyalikh DV, Huo J, Song H, et al. Effect of oxidation and heat treatment on the morphology and electronic structure of carbon-encapsulated iron carbide nanoparticles. *Materials Chemistry and Physics*. 2012;135(1):235-40.
- [44] Du Y, Liu W, Qiang R, Wang Y, Han X, Ma J, et al. Shell thickness-dependent microwave absorption of core-shell Fe₃O₄@C composites. *ACS applied materials & interfaces*. 2014;6(15):12997-3006.
- [45] Caçado LG, Takai K, Enoki T, Endo M, Kim YA, Mizusaki H, et al. Measuring the degree of stacking order in graphite by Raman spectroscopy. *Carbon*. 2008;46(2):272-5.
- [46] Bystrzejewski M, Karoly Z, Szepvolgyi J, Kaszuwara W, Huczko A, Lange H. Continuous synthesis of carbon-encapsulated magnetic nanoparticles with a minimum production of amorphous carbon.

Carbon. 2009;47(8):2040-8.

- [47] Xiang J, Li J, Zhang X, Ye Q, Xu J, Shen X. Magnetic carbon nanofibers containing uniformly dispersed Fe/Co/Ni nanoparticles as stable and high-performance electromagnetic wave absorbers. *J Mater Chem A*. 2014;2(40):16905-14.
- [48] Wu W, Zhu Z, Liu Z, Xie Y, Zhang J, Hu T. Preparation of carbon-encapsulated iron carbide nanoparticles by an explosion method. *carbon*. 2003;41(2):317-21.
- [49] Huo J, Song H, Chen X, Zhao S, Xu C. Structural transformation of carbon-encapsulated iron nanoparticles during heat treatment at 1000 degrees C. *Materials Chemistry and Physics*. 2007;101(1):221-7.
- [50] Qiu J, Li Q, Wang Z, Sun Y, Zhang H. CVD synthesis of coal-gas-derived carbon nanotubes and nanocapsules containing magnetic iron carbide and oxide. *Carbon*. 2006;44(12):2565-8.
- [51] Qiang R, Du Y, Chen D, Ma W, Wang Y, Xu P, et al. Electromagnetic functionalized Co/C composites by in situ pyrolysis of metal-organic frameworks (ZIF-67). *Journal of Alloys and Compounds*. 2016;681:384-93.
- [52] Zhang B, Du Y, Zhang P, Zhao H, Kang L, Han X, et al. Microwave absorption enhancement of Fe₃O₄/polyaniline core/shell hybrid microspheres with controlled shell thickness. *Journal of Applied Polymer Science*. 2013;130(3):1909-16.
- [53] Ilkiv B, Petrovska S, Sergiienko R, Foya O, Ilkiv O, Shibata E, et al. Synthesis, characterization and X-ray spectral investigation of hollow graphitic carbon nanospheres. *Journal of Alloys and Compounds*. 2014;617:616-21.
- [54] Rong Cb, Li D, Nandwana V, Poudyal N, Ding Y, Wang ZL, et al. Size-Dependent Chemical and Magnetic Ordering in L10-FePt Nanoparticles. *Advanced Materials*. 2006;18(22):2984-8.
- [55] Wen B, Cao M, Lu M, Cao W, Shi H, Liu J, et al. Reduced graphene oxides: light-weight and high-efficiency electromagnetic interference shielding at elevated temperatures. *Adv Mater*. 2014;26(21):3484-9.
- [56] Bystrzejewski M, Huczko A, Lange H, Cudziło S, Kiciński W. Combustion synthesis route to carbon-encapsulated iron nanoparticles. *Diamond and Related Materials*. 2007;16(2):225-8.
- [57] Yan SJ, Xu CY, Jiang JT, Liu DB, Wang ZY, Tang J, et al. Strong dual-frequency electromagnetic absorption in Ku-band of C@FeNi₃ core/shell structured microchains with negative permeability. *Journal of Magnetism and Magnetic Materials*. 2014;349:159-64.
- [58] Liu W, Zhong W, Jiang HY, Tang NJ, Wu XL, Du WY. Synthesis and magnetic properties of FeNi₃/Al₂O₃ core-shell nanocomposites. *The European Physical Journal B*. 2005;46(4):471-4.
- [59] Liu Q, Cao Q, Bi H, Liang C, Yuan K, She W, et al. CoNi@SiO₂@TiO₂ and CoNi@Air@TiO₂ Microspheres with Strong Wideband Microwave Absorption. *Adv Mater*. 2016;28(3):486-90.
- [60] Lv H, Ji G, Zhang H, Li M, Zuo Z, Zhao Y, et al. CoxFey@C Composites with Tunable Atomic Ratios for Excellent Electromagnetic Absorption Properties. *Scientific reports*. 2015;5:18249-59.
- [61] Yu H, Wang T, Wen B, Lu M, Xu Z, Zhu C, et al. Graphene/polyaniline nanorod arrays: synthesis and excellent electromagnetic absorption properties. *Journal of Materials Chemistry*. 2012;22:21679-85.